

DOI:10.1002/ejic.201402286

## Synthesis and Characterization of Spirosilanes – 1,2-Hydroboration and 1,1-Carboboration

Ezzat Khan,<sup>\*[a]</sup> Bernd Wrackmeyer,<sup>[b]</sup> Cristian Döring,<sup>[b]</sup> and Rhett Kempe<sup>[b]</sup>

**Keywords:** Spiro compounds / Hydroboration / Carboboration / Silanes / Structure elucidation

Starting from dichloro(divinyl)silane, the dialkynyl(divinyl)silanes  $(\text{CH}_2=\text{CH})_2\text{Si}(\text{C}\equiv\text{CR})_2$  ( $\text{R} = t\text{Bu}$ , *p*-tolyl, 3-thienyl,  $\text{CH}_2\text{NMe}_2$ ) were prepared. These silanes were treated with 9-borabicyclo[3.3.1]nonane (9-BBN) for 1,2-hydroboration of the vinyl groups. The hydroboration products rearranged quickly and quantitatively by intramolecular 1,1-carboboration into the respective target compounds, the axially chiral 5-silaspiro[4.4]nona-1,6-dienes bearing boryl groups at the 2- and 7-positions and the R substituents at the 1- and 6-positions.

Simple protodeborylation with acetic acid proved possible, except for  $\text{R} = t\text{Bu}$ . The remaining Si–C function in  $(\text{CH}_2=\text{CH})_2\text{Si}(\text{Cl})\text{C}\equiv\text{C}t\text{Bu}$  opens the way to new spiro silanes after a sequence of hydroboration/carboboration/hydroboration, for which a first example was studied. The products were characterized by X-ray diffraction in the solid state and NMR spectroscopy in solution ( $^1\text{H}$ ,  $^{11}\text{B}$ ,  $^{13}\text{C}$ ,  $^{15}\text{N}$ ,  $^{29}\text{Si}$ ), complemented by optimization of gas-phase structures and calculation of NMR parameters by DFT methods.

### Introduction

1,1-Carboboration and more recently the combination of 1,2-hydroboration and 1,1-carboboration have opened attractive routes to Group 14 metallacycles.<sup>[1–3]</sup> With silicon, heterocycles such as 1-silacyclobutenes,<sup>[4–6]</sup> 1-silacyclopent-2-enes,<sup>[7,8]</sup> 1-silacyclohex-2-enes,<sup>[7,9]</sup> and silole derivatives are particularly noteworthy.<sup>[10–12]</sup> Addressing 1-silacyclopent-2-enes, numerous derivatives bearing functionalities such as Si–organyl, Si–Cl, and Si–H at a chiral silicon atom have become available (Figure 1, example A). The processes of 1,2-hydroboration<sup>[13]</sup> and 1,1-carboboration<sup>[14]</sup> are simple, efficient, and cost effective. Although they require careful purification of the starting silanes, the following reactions afford the desired pure products in high yield.

In addition to simple silicon heterocycles, a few examples of silane derivatives with the silicon atom in the center of a spiro structure have been reported.<sup>[15–19]</sup> Most routes towards spiro silanes appear to be rather inconvenient and narrow, particularly if the rings contain C=C bonds or other functional groups attached to the carbon atoms of the ring. Recently, we have characterized a few spiro silane derivatives as first examples, namely, the 4-silaspiro[3.3]hepta-1,5-dienes<sup>[20]</sup> and the axially chiral 5-silaspiro[4.4]nona-1,6-dienes (Figure 1, example B),<sup>[21]</sup> through consecutive 1,2-hydroboration and 1,1-carboboration reactions. The combination of these stereo- and regioselective reac-

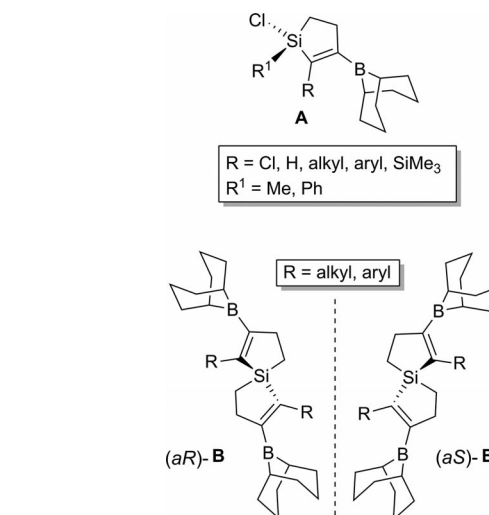


Figure 1. Examples of 1-silacyclopent-2-ene derivatives A and B.

tions appears to be versatile in synthesis.<sup>[4–9,20,21]</sup> In the present work, further examples are given to emphasize the simple and general route to 5-silaspiro[4,4]nona-1,6-diene derivatives. Furthermore, a route to other types of spiro silanes containing the 1-silacyclopent-2-ene unit is explored.

### Results and Discussion

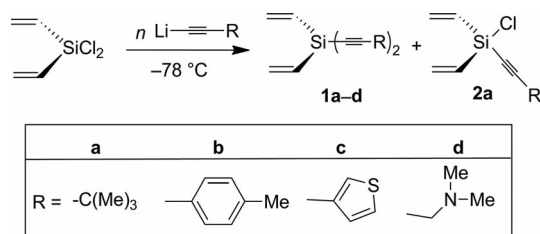
#### Synthesis of Starting Silanes

Divinyl(dichloro)silane was treated with 2 equiv. of the respective lithiated alkyne at low temperature ( $-78\text{ }^\circ\text{C}$ )<sup>[22–24]</sup>

[a] Department of Chemistry, University of Malakand, 18550 Chakdara, Khyber Pakhtunkhwa, Pakistan  
E-mail: ekhan@uom.edu.pk  
www.uom.edu.pk

[b] Anorganische Chemie II, Universität Bayreuth, 95440 Bayreuth, Germany

to afford the required dialkynyl(divinyl)silanes **1**. For the *t*Bu derivative, the reaction afforded a mixture of **1a** and **2a** (Scheme 1). The components of the mixture were separated by fractional distillation under vacuum (ca.  $10^{-3}$  Torr). The purity of the new dialkynyl(divinyl)silanes was checked by NMR spectroscopy (see Exp. Section), and the compounds were used in further reactions when the required purity ( $\geq 99\%$ ) was achieved. The substituents R were selected to provide a bulky alkyl group (**1a** and **2a**), an aryl group (**1b**),



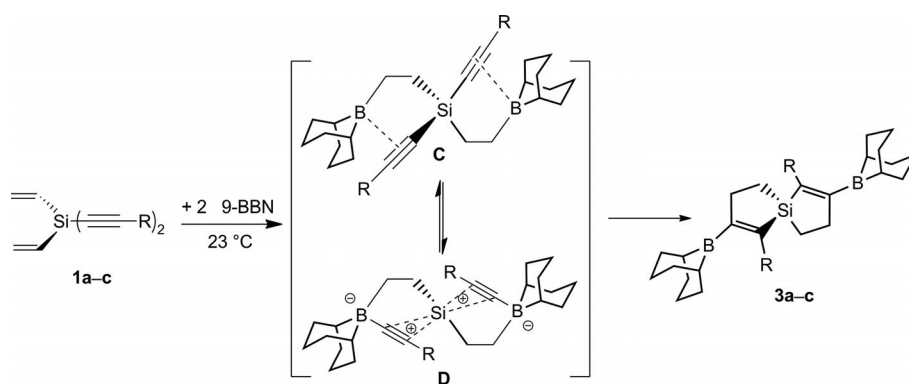
Scheme 1. Syntheses of dialkynyl(divinyl)silanes **1a–1d** and alkynyl(divinyl)silane **2a**.

a heteroaryl group (**1c**), and a potentially coordinating Lewis base (**1d**).

### 1,2-Hydroboration and 1,1-Carboboration

The dialkynyl(divinyl)silanes **1a–1d** fulfill all of requirements to combine 1,2-hydroboration and 1,1-organoboration for the syntheses of spiro-silanes of type **B**.<sup>[21]</sup> In the present study, it is shown that different substituents R do not have an appreciable influence on the course of the reactions, which consist of twofold intermolecular 1,2-hydroborations and twofold intramolecular 1,1-vinylborations. All of the reactions were performed by following the literature procedure,<sup>[7,8,21]</sup> and the required products were obtained in reasonable quantity and with sufficient purity of  $>98\%$  (Scheme 2).

The proposed mechanism of the reaction for the synthesis of the spiro-silanes given in Scheme 2 has already been discussed in greater detail,<sup>[21]</sup> supported by theoretical cal-



Scheme 2. Syntheses of spiro-silanes bearing *t*Bu, 4-Me-C<sub>6</sub>H<sub>4</sub>, and 3-thienyl substituents at the 1- and 6-positions.

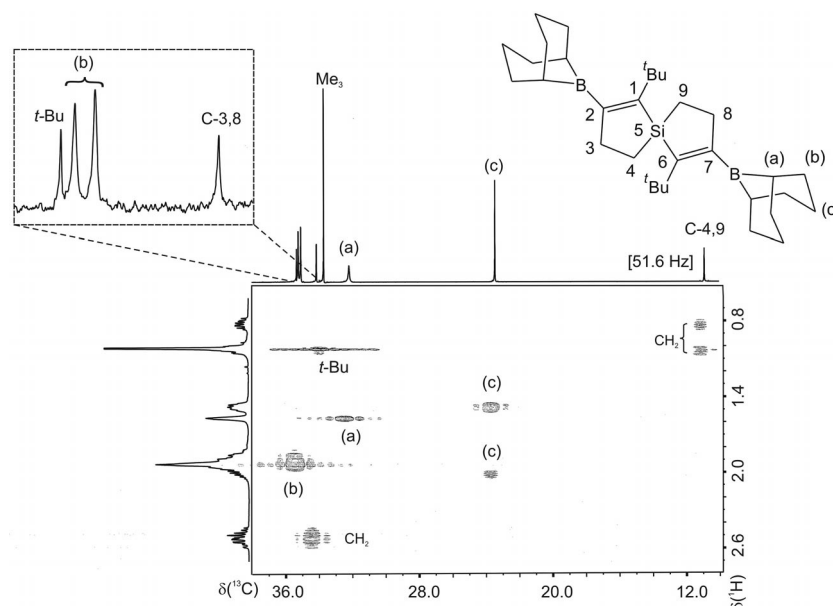


Figure 2. Contour plot of (part of the aliphatic region) the 2D <sup>1</sup>H–<sup>13</sup>C correlated spectrum of spiro-silane **3a** [recorded by the gradient-selected heteronuclear single quantum coherence (gs)HSQC method].<sup>[27]</sup>

culations.<sup>[25]</sup> In a first step, silanes bearing vinyl and alkynyl groups at the Si atom react with 9-borabicyclo[3.3.1]nonane (9-BBN) selectively by 1,2-hydroboration of the C=C bond, and the boron atom preferably becomes linked to the terminal carbon atom of the vinyl group (intermediate **C**, Scheme 2). This is a unique property of 9-BBN, which prefers the terminal C=C bond over the C≡C bond, if we compare it with other dialkylboranes.<sup>[26]</sup> The first intermediate **C** (not observed) from twofold 1,2-hydroborations possesses a suitable geometry for intramolecular 1,1-vinylboration. In the next step, an interaction between the electron-deficient boron atoms and the C≡C units (Si–C activation indicated by dashed lines) causes cleavage of the Si–C≡ bonds and the formation of a zwitterionic alkynylborate-like intermediate **D** (not detected). Finally 1,1-vinylboration leads to the spiro silane by twofold ring closure.<sup>[21]</sup> Usually, the intermolecular 1,1-organoboration of alkynylsilanes with trialkylboranes (BR<sub>3</sub>) requires harsh conditions and long reaction times.<sup>[14]</sup> By contrast, the intramolecular 1,1-organoboration proceeds quickly and more smoothly, as studied for vinylsilanes.<sup>[7,8,21]</sup> The results of the present study lead us to conclude that the consecutive 1,2-hydroboration and 1,1-vinylboration reactions proceed smoothly and selectively independent of the R group. All of the spiro silanes bearing boryl groups at the 2- and 7-positions were colorless oily or crystalline materials, and their structures could be deduced from a consistent set of solution-state NMR spectroscopic data (Figure 2 and Table 1) and also by X-ray diffraction (Figures 3 and 4).

Table 1. <sup>13</sup>C, <sup>11</sup>B, and <sup>29</sup>Si NMR spectroscopic data<sup>[a]</sup> of spiro silane derivatives **3–5**.

	$\delta^{13}\text{C}$ (C-1,6)	$\delta^{13}\text{C}$ (C-2,7)	$\delta^{13}\text{C}$ (C-3,8)	$\delta^{13}\text{C}$ (C-4,9)	$\delta^{11}\text{B}$	$\delta^{29}\text{Si}$
<b>3a</b> <sup>[b]</sup>	151.0 (59.9)	167.2 br.	34.1	10.9 (51.6)	85.1	32.8
<b>3b</b> <sup>[c]</sup>	149.8 (59.0)	172.4 br.	35.3	9.3 (51.8)	84.4	36.3
<b>3c</b> <sup>[d]</sup>	143.0 (59.3)	173.2 br.	34.9	8.9 (51.8)	85.4	37.0
<b>4d</b> <sup>[e]</sup>	132.4 (64.8)	194.6 br.	35.9	11.3 (53.1)	6.9	17.8
<b>5b</b> <sup>[f]</sup>	142.2 (60.8)	148.2 (11.4)	31.1	8.0 (50.5)	–	29.8
<b>5c</b> <sup>[g]</sup>	136.3 (61.1)	148.3 (11.0)	31.1	7.5 (52.3)	–	30.2

[a] NMR spectroscopic data measured in C<sub>6</sub>D<sub>6</sub> at 23 ± 1 °C, the values in brackets represent coupling constants <sup>1</sup>J<sub>29Si,13C</sub> and <sup>2</sup>J<sub>29Si,13C</sub> [Hz], br. stands for a broad <sup>13</sup>C signal owing to partially relaxed <sup>13</sup>C–<sup>11</sup>B spin–spin coupling.<sup>[28]</sup> [b] Measured in CDCl<sub>3</sub>, other <sup>13</sup>C NMR spectroscopic data:  $\delta$  = 33.7 (Me), 35.3 (*t*Bu), 35.1, 35.2, 32.2 (br), 23.4 (9-BBN) ppm. [c] Other <sup>13</sup>C NMR spectroscopic data:  $\delta$  = 34.4, 34.9, 32.6 (br), 23.8 (9-BBN), 140.8 (<sup>29</sup>J<sub>Si,13C</sub> = 6.1 Hz), 129.2, 128.3, 135.8, 21.1 (4-Me-C<sub>6</sub>H<sub>4</sub>) ppm. [d] Other <sup>13</sup>C NMR spectroscopic data:  $\delta$  = 34.3, 34.7, 32.6 (br), 23.7 (9-BBN), 144.4 (<sup>29</sup>J<sub>Si,13C</sub> = 6.9 Hz), 128.0, 125.7, 120.3 (3-thienyl) ppm. [e] Other <sup>13</sup>C NMR spectroscopic data:  $\delta$  = 69.9 (<sup>29</sup>J<sub>Si,13C</sub> = 11.0 Hz, NCH<sub>2</sub>), 48.7 (Me), 48.6 (Me), 34.2, 34.1, 30.6, 30.5, 24.3, 24.0, 22.4 (br), 22.1 (br., 9-BBN) ppm. [f] Other <sup>13</sup>C NMR spectroscopic data:  $\delta$  = 21.1, 137.4 (<sup>29</sup>J<sub>Si,13C</sub> = 5.3 Hz), 129.6, 126.9, 136.2 (Me, *i*-, *o*-, *m*-, *p*-4-Me-C<sub>6</sub>H<sub>4</sub>) ppm. [g] Other <sup>13</sup>C NMR spectroscopic data:  $\delta$  = 141.4 (<sup>29</sup>J<sub>Si,13C</sub> = 5.4 Hz), 126.1, 125.7, 120.7 (3-thienyl) ppm.

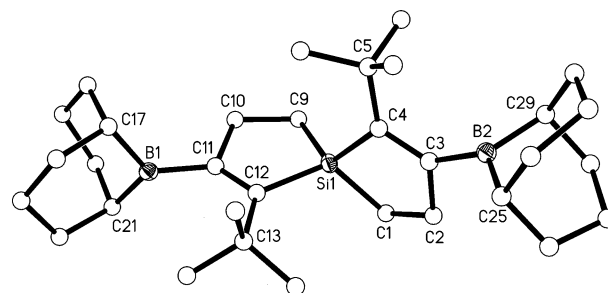


Figure 3. Molecular structure of spiro silane **3a**. Drawn at 40% probability level; hydrogen atoms are omitted for clarity; see Table 2 for selected bond lengths and angles.

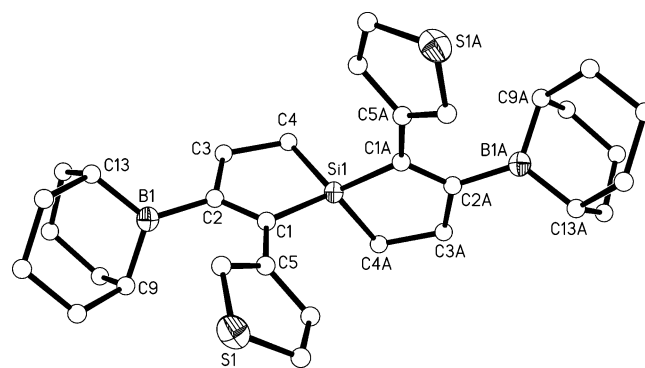
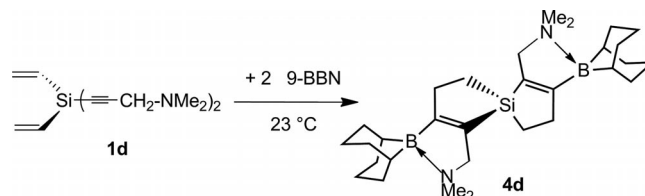


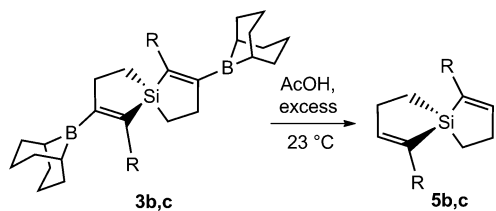
Figure 4. Molecular structure of spiro silane **3c**. Drawn at 40% probability level; hydrogen atoms are omitted for clarity; see Table 2 for selected bond lengths and angles.

For **1d**, derived from propargylamine, the reaction with 2 equiv. of 9-BBN proceeded in the same way as those of **1a–1c**. The major difference in the final polycyclic product **4d** arises from coordinative N–B bonding (Scheme 3), as deduced from the <sup>11</sup>B and <sup>29</sup>Si NMR spectroscopic data (see below). Compound **4d** is a white, amorphous powder.



Scheme 3. Synthesis of the polycyclic spiro silane derivative **4d**.

The spiro silane derivatives discussed so far contain boryl groups. As they are active functional groups, they invite further chemistry such as oxidation, hydrolysis, or Suzuki-type coupling reactions.<sup>[29]</sup> Here, we describe the protodeborylation of **3b** and **3c** as representative examples. The treatment of **3b** and **3c** with an excess of glacial acetic acid by the literature procedure<sup>[30]</sup> afforded the desired protodeborylated spiro silanes (Scheme 4). Compounds **5b** and **5c** were obtained as crystalline materials, and the structure of **5b** (Figure 5) was determined by X-ray diffraction (see below). The same reaction to remove the boryl substituents failed for **3a**, presumably owing to the bulk of the *t*Bu group.



Scheme 4. Protodeborylation of the spirosilanes **3b** and **3c** with an excess of acetic acid.

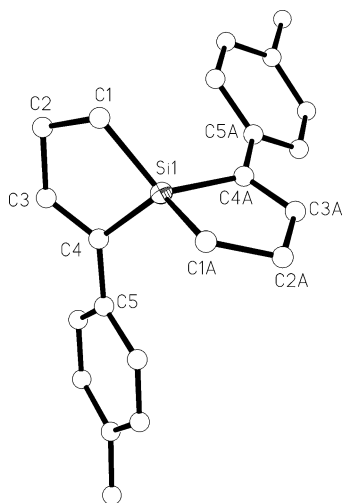
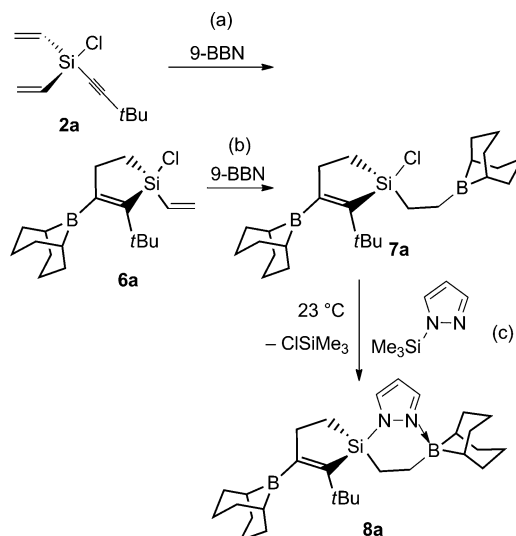


Figure 5. Molecular structure of spirosilane **5b**, an example of a protodeborylated spirosilane. Drawn at 50% probability level; hydrogen atoms are omitted for clarity. See Table 2 for selected bond lengths and angles.

### A New Spirosilane

The 1,2-hydroboration and 1,1-carboboration of **2a** leads to the 1-silacyclopent-2-ene derivative **6a** with Si–vinyl and Si–Cl functions (Scheme 5, a), both of which enhance its



Scheme 5. Stepwise synthesis of spirosilane **8a**.

synthetic potential. Thus, another equivalent of 9-BBN can still be reacted to afford 1-silacyclopent-2-ene derivative **7a** (Scheme 5, b), which now contains Si–Cl and C–B functionalities. In a first attempt to make use of these functions, the nonagostic complex **7a** was treated with *N*-(trimethylsilyl)pyrazole at ambient temperature (Scheme 5, c). The reaction proceeded by elimination of Me<sub>3</sub>SiCl, and new Si–N and B–N bonds were formed to give the spirosilane **8a** in high purity (>99%). The structure of **8a** in solution follows from the NMR spectroscopic data (<sup>1</sup>H, <sup>13</sup>C, <sup>15</sup>N, <sup>11</sup>B, and <sup>29</sup>Si) and was confirmed by single-crystal X-ray diffraction (see below).

### NMR spectroscopy and DFT Calculations

All of the NMR spectroscopic data (Table 1 and Exp. Section) strongly support the proposed solution-state structures, including the persistence of the axial chirality of the 5-silaspiro[4.4]nona-1,6-dienes. The latter is shown by the splitting of the relevant <sup>1</sup>H and <sup>13</sup>C NMR signals (shown for some examples in Figure 2). Other convincing arguments for the structural assignments such as the <sup>11</sup>B, <sup>13</sup>C, and <sup>29</sup>Si chemical shifts and spin–spin coupling constants, in particular <sup>n</sup>J<sub>29Si,13C</sub>, have been discussed previously for related derivatives.<sup>[21]</sup> As the X-ray diffraction studies indicated negligible intermolecular interactions, the comparison between calculated gas-phase structures and direct structural evidence from the solid state is meaningful. Therefore, the geometries of the gas-phase structures of **3**, **4**, **5**, and **8a** were optimized at the B3LYP/6-311+(G/d,p) level of theory,<sup>[31]</sup> and satisfactory agreement was observed. This prompted us to calculate some chemical shifts<sup>[32]</sup> and coupling constants,<sup>[33]</sup> in particular δ<sup>11</sup>B, δ<sup>15</sup>N, and δ<sup>29</sup>Si as well as <sup>n</sup>J<sub>29Si,13C</sub> at the same level of theory. Again the agreement with the experimental data was encouraging. This is well known for δ<sup>11</sup>B<sup>[34]</sup> and appears to be helpful with δ<sup>29</sup>Si<sup>[35]</sup> [in the present case, the increased <sup>29</sup>Si nuclear shielding in **4d** (δ<sup>29</sup>Si = 17.8 ppm) is correctly predicted] and it serves to assign the different <sup>15</sup>N NMR signals of **8a** to the Si–N (δ<sup>15</sup>N = –165.2 ppm) and B–N (δ<sup>15</sup>N = –117.7 ppm) bonds. As shown recently for other 1-silacyclopent-2-enes,<sup>[8b]</sup> the sign and magnitude of calculated <sup>n</sup>J<sub>29Si,13C</sub> coupling constants correspond closely to the experimental data.<sup>[35]</sup>

### X-ray Structural Analyses of 3a, 3c, 5b, and 8a

The molecular structures of silanes **3a**, **3c**, **5b**, and **8a** are represented in Figures 3–6. The structural data pertinent to **3a**, **3c**, and **5b** compare well with the reported structures, and there is a negligible influence of the R group. All bond lengths and angles (Table 2) are within the expected ranges.<sup>[21]</sup> In **3a**, the carbon atoms around the silicon atom are arranged in a distorted tetrahedral fashion with the expected small endocyclic C1–Si1–C4 angle of 92.7°. The geometry around the boron atoms is close to trigonal planar. The distortion seems to be caused by the proximity to the

Table 2. Selected bond lengths [pm] and angles [°] of boryl-substituted spirosilanes **3a** and **3c** and protodeborylated spirosilane **5b**.

<b>3a</b> (R = <i>t</i> Bu)		<b>3c</b> (R = 3-thienyl)		<b>5b</b> (R = 4-Me-C <sub>6</sub> H <sub>4</sub> )	
C1–Si1	187.5(15)	C4–Si1	187.4(3)	C1–Si1	187.8(3)
C4–Si1	187.3(13)	C1–Si1	186.8(2)	C4–Si1	187.6(3)
C1–C2	154.0(2)	C3–C4	154.1(3)	C1–C2	154.9(4)
C2–C3	153.8(19)	C2–C3	152.6(3)	C2–C3	150.8(4)
C3–C4	135.2(2)	C1–C2	135.7(3)	C3–C4	134.6(4)
C3–B2	156.5(2)	C2–B1	156.4(4)	–	–
C4–C5	153.6(18)	C1–C5	146.3(3)	C4–C5	148.3(4)
C2–C1–Si1	105.5(9)	C3–C4–Si1	106.58(17)	C2–C1–Si1	105.4(2)
C3–C2–C1	110.8(11)	C2–C3–C4	112.0(2)	C3–C2–C1	109.9(2)
C4–C3–C2	116.5(12)	C1–C2–C3	116.5(2)	C4–C3–C2	120.1(3)
C4–C3–B2	129.5(12)	C1–C2–B1	124.7(2)	–	–
C3–C4–Si1	110.6(10)	C2–C1–Si1	111.30(18)	C3–C4–Si1	108.4(2)
C5–C4–Si1	126.1(10)	C5–C1–Si1	126.81(18)	C5–C4–Si1	128.5(2)
C1–Si1–C4	92.7(6)	C1–Si1–C4	119.82(11)	C1–Si1–C4	119.9(13)
C1–Si1–C9	115.0(7)	C1–Si1–C1A	118.30(16)	C1–Si1–C1	118.7(2)
C1–Si1–C12	119.7(6)	C4–Si1–C1A	93.16(11)	C4–Si1–C1	93.6(13)
C4–Si1–C9	119.7(6)	C1–Si1–C4A	93.16(11)	C1–Si1–C4	119.9(13)

*t*Bu group. Both five-membered rings of the molecule are considerably twisted with Si1–C9–C10–C11 and Si1–C1–C2–C3 torsion angles of –14.1 and –19.2°, respectively. The silicon and boron atoms are *trans* to each other and are almost coplanar at the C=C bonds (torsion angles: B1–C11–C12–Si1 174.7°, B2–C3–C4–Si1 175.2°). The same features were observed in the molecular structure of **3c**.

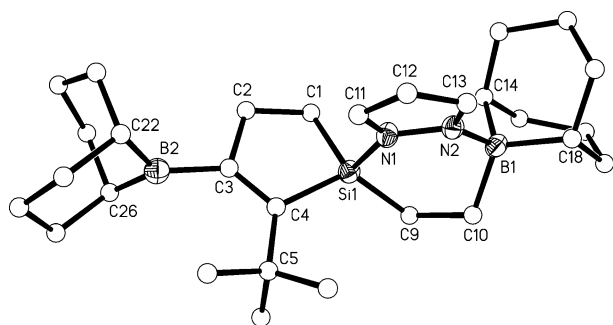


Figure 6. Molecular structure of spirosilane derivative **8a**. Drawn at 40% probability level; hydrogen atoms are omitted for clarity. Selected bond lengths [pm] and angles [°]: C1–C2 154.4(2), C1–Si1 185.4(19), C2–C3 153.1(3), C3–C4 135.6(2), C3–B2 157.2(3), C4–C5 152.8(2), C4–Si1 186.7(17), C9–C10 155.2(2), C9–Si1 185.9(19), C10–B1 164.2(3), N1–Si1 181.7(14), N2–B1 162.7(2); C4–C3–C2 117.08(15), C4–C3–B2 130.9(16), C3–C4–Si1 108.79(13), N1–Si1–C1 108.30(8), N1–Si1–C9 104.38(7), C1–Si1–C9 119.49(9), N1–Si1–C4 104.50(7), C1–Si1–C4 94.99(8), C9–Si1–C4 123.8(8).

The molecular structure of **5b** is shown in Figure 5, it has a distorted tetrahedral geometry around the silicon atom with bond angles of 93.6, 119.9, 118.7, and 113.3°. The five-membered rings of the spiro structure are slightly distorted with respect to a plane (torsion angles: Si1–C1–C2–C3 16.5° and Si1–C4–C3–C2 –0.7°). The *p*-tolyl moieties are twisted by 31° with respect to the five-membered rings of the spiro structure. All other bond lengths and angles are within the expected ranges.

The molecular structure of **8a** suffers from a little disorder, but it can be solved unambiguously (Figure 6). The data obtained for the five-membered 1-silacyclopent-2-ene ring are within the expected range.<sup>[5,8,21]</sup> The silicon atom has two different ring structures at either side, and its surroundings correspond to a distorted tetrahedron, as expected (bond angles: N1–Si1–C9 104.4°, C1–Si1–C4 95.0°, C1–Si1–N1 108.3°, and C4–Si1–C9 123.8°). The molecule bears two boron centers, one is tricoordinate, and the other is tetracoordinate. All of the carbon atoms attached to the B2 center adopt trigonal planar surroundings with bond angles of C26–B2–C3 124.2°, C22–B2–C3 123.3°, and C22–B2–C26 110.5°. The four-coordinate boron atom adopts a tetrahedral geometry with bond angles of N2–B1–C10 103.0°, C18–B1–C14 104.8°, N2–B1–C18 110.1°, and C10–B1–C14 113.7°.

All positions of the atoms of the five-membered rings deviate slightly from a plane with torsion angles of Si1–C1–C2–C3 15.8° and Si–C4–C3–C2 1.9°. The six-membered ring containing the silicon atom is markedly nonplanar as far as the Si1–C9–C10–B1 unit is concerned (torsion angle –47.9°). By contrast, the atoms in the fragment Si1–N1–N2–B1 almost form a plane (torsion angle 7.4°).

## Conclusions

Axially chiral 5-silaspiro[4.4]nona-1,6-dienes bearing boryl groups at the 2- and 7-positions and various R substituents at the 1- and 6-positions are accessible in essentially quantitative yield by combining consecutive intermolecular 1,2-hydroboration and intramolecular 1,1-carbo-boration reactions; the results were fairly independent of the R group. In the absence of extreme steric hindrance, protodeborylation with acetic acid can be achieved by following a simple protocol. The products, including a new spirosilane, were characterized in the solid state by X-ray diffraction and in solution by multinuclear magnetic reso-

nance techniques; in addition, the gas-phase structures were optimized by DFT methods, which also served for the calculation of NMR spectroscopic parameters.

## Experimental Section

**General:** All preparative work and the handling of air- and moisture-sensitive chemicals were performed under a dry argon atmosphere. Dialkyn-1-ylsilanes were prepared and purified by following the reported procedures<sup>[13,14]</sup> and fully characterized by multinuclear NMR spectroscopy. Other commercial chemicals such as dichloro(divinyl)silane, *n*-butyllithium (1.6 M in hexane), propargylamine, pyrazole, 9-borabicyclo[3.3.1]nonane, and glacial acetic acid were used as received without further purification. The NMR spectra were recorded at 23 ± 1 °C with Varian Inova 300 and 400 spectrometers and a Bruker AMX 500 spectrometer (<sup>15</sup>N NMR), all equipped with multinuclear units; C<sub>6</sub>D<sub>6</sub> or CDCl<sub>3</sub> solutions (ca. 10–15% v/v) in 5 mm o.d. tubes were used. Chemical shifts (in ppm) are given relative to SiMe<sub>4</sub> [TMS; δ<sup>1</sup>H (C<sub>6</sub>D<sub>5</sub>H) = 7.15 ppm, δ<sup>13</sup>C (C<sub>6</sub>D<sub>6</sub>) = 128.0 ppm, δ<sup>1</sup>H (CHCl<sub>3</sub>) = 7.23 ppm, δ<sup>13</sup>C (CDCl<sub>3</sub>) = 77.0 ppm, δ<sup>29</sup>Si = 0 ppm for SiMe<sub>4</sub> with Ξ(<sup>29</sup>Si) = 19.867187 MHz], MeNO<sub>2</sub> (neat) for <sup>15</sup>N [Ξ(<sup>15</sup>N) = 10.136767 MHz], and BF<sub>3</sub>·OEt<sub>2</sub> for <sup>11</sup>B [δ<sup>11</sup>B = 0 ppm with Ξ(<sup>11</sup>B) = 32.083971 MHz]. The <sup>29</sup>Si NMR spectra were recorded by using the refocused insensitive nuclei enhanced by polarization transfer (INEPT) pulse sequence with <sup>1</sup>H decoupling<sup>[21]</sup> based on <sup>n</sup>J<sub>Si,1H<sub>vinyl</sub> ≈ 12–20 Hz (*n* = 2,3) and <sup>3</sup>J<sub>Si,1H(C<sup>4</sup>) ≈ 25 Hz (after optimization of the respective refocusing delays). Melting points were determined by using a Büchi 510 melting point apparatus.</sub></sub>

All quantum chemical calculations were performed by using the Gaussian 09 program package.<sup>[36]</sup> The optimized geometries at the B3LYP/6-311+G(d,p) level of theory<sup>[31]</sup> were found to be minima by the absence of imaginary frequencies. The NMR parameters were calculated<sup>[32,33]</sup> at the same level of theory. The calculated nuclear magnetic shielding constants σ<sup>11</sup>B were converted by δ<sup>11</sup>B(calcd.) = σ(<sup>11</sup>B) – σ(<sup>11</sup>B, B<sub>2</sub>H<sub>6</sub>) with σ(<sup>11</sup>B, B<sub>2</sub>H<sub>6</sub>) = +84.1 [δ<sup>11</sup>B(B<sub>2</sub>H<sub>6</sub>) = 18 and δ<sup>11</sup>B (BF<sub>3</sub>·OEt<sub>2</sub>) = 0] and the calculated σ(<sup>29</sup>Si) values were converted to chemical shifts δ<sup>29</sup>Si by δ<sup>29</sup>Si (calcd.) = σ(<sup>29</sup>Si, TMS) – σ(<sup>29</sup>Si) with σ(<sup>29</sup>Si, TMS) = +340.1 and δ<sup>29</sup>Si(TMS) = 0.

**Dialkyn-1-yldivinylsilanes 1a–1d and Dialkyn-1-ylvinylsilane 2a:** A suspension of LiC≡C*t*Bu (20 mmol, in pentane) was prepared at –78 °C. To this suspension at the same temperature, an equimolar amount of dichlorodivinylsilane was added. The reaction mixture was stirred for 1 h and then warmed to room temperature. The solid material (LiCl) was removed by filtration, and all volatiles were removed under reduced pressure (20 Torr). The remaining oily residue was identified as a mixture of **1a**, **2a**, and some amount of unreacted silane. Pure samples of **1a** and **2a** were obtained by fractional distillation. The other silanes **1b**, **1c**, and **1d** were prepared and purified in the same way.

**1a:** Yield 65%. <sup>1</sup>H NMR (400 MHz, C<sub>6</sub>D<sub>6</sub>): δ = 1.0 (s, 18 H, *t*Bu), 6.0 (dd, *J*<sub>H,1H</sub> = 6.6, 11.3 Hz, 2 H, SiCH=), 6.2 (m, 4 H, =CH<sub>2</sub>) ppm. <sup>13</sup>C NMR: δ = 76.5 (*J*<sub>Si,13C</sub> = 106.6 Hz, SiC≡), 118.5 (*J*<sub>Si,13C</sub> = 19.5 Hz, ≡C), 134.1 (*J*<sub>Si,13C</sub> = 81.6 Hz, SiC=), 135.2 (=C), 28.4, 30.8 (*t*Bu) ppm. <sup>29</sup>Si NMR: δ = –53.9 ppm.

**1b:** Yield 96%. <sup>1</sup>H NMR (400 MHz, C<sub>6</sub>D<sub>6</sub>): δ = 6.1 (m, *J*<sub>H,1H</sub> = 9.0 Hz, 1 H, SiCH), 6.4 (m, *J*<sub>H,1H</sub> = 9.4, 8.3 Hz, 2 H, H<sub>2</sub>C=), 1.9, 6.7, 7.3 (s, m, m, 7 H, 4-Me-C<sub>6</sub>H<sub>4</sub>) ppm. <sup>13</sup>C NMR: δ = 87.1 (*J*<sub>Si,13C</sub>

= 105.5 Hz, SiC≡), 109.0 (*J*<sub>Si,13C</sub> = 20.2 Hz, ≡C), 132.9 (*J*<sub>Si,13C</sub> = 82.1 Hz, SiC=), 136.4 (=C), 119.9, 132.4, 129.3, 139.4, 21.3 (4-Me-C<sub>6</sub>H<sub>4</sub>) ppm. <sup>29</sup>Si NMR: δ = –52.8 ppm.

**1c:** Yield 98%. <sup>1</sup>H NMR (400 MHz, C<sub>6</sub>D<sub>6</sub>): δ = 6.1 (m, 2 H, SiCH=), 6.3 (m, 4 H, =CH<sub>2</sub>), 6.6, 6.9, 7.1 (m, m, m, 6 H, 3-thienyl) ppm. <sup>13</sup>C NMR: δ = 87.5 (*J*<sub>Si,13C</sub> = 104.9 Hz, SiC≡), 103.7 (*J*<sub>Si,13C</sub> = 20.2 Hz, ≡C), 132.5 (*J*<sub>Si,13C</sub> = 82.3 Hz, SiC=), 136.6 (=C), 131.1, 130.1, 125.5, 122.0 (3-thienyl) ppm. <sup>29</sup>Si NMR: δ = –52.8 ppm.

**1d:** Yield 97%. <sup>1</sup>H NMR (400 MHz, CDCl<sub>3</sub>): δ = 2.14, 3.17 (s, s, 16 H, CH<sub>2</sub>NMe<sub>2</sub>), 5.94–6.00 (m, 6 H, Si–vinyl) ppm. <sup>13</sup>C NMR: δ = 82.8 (*J*<sub>Si,13C</sub> = 104.2 Hz, SiC≡), 104.0 (*J*<sub>Si,13C</sub> = 19.3 Hz, ≡C), 132.0 (*J*<sub>Si,13C</sub> = 81.8 Hz, SiC=), 135.6 (=C), 43.7 (Me), 48.5 (CH<sub>2</sub>) ppm. <sup>29</sup>Si NMR: δ = –54.3 ppm.

**2a:** Yield 30%; b.p. 32–35 °C/0.1 Torr. <sup>1</sup>H NMR (400 MHz, C<sub>6</sub>D<sub>6</sub>): δ = 1.0 (s, 9 H, *t*Bu), 6.0 (dd, *J*<sub>H,1H</sub> = 6.5, 11.4 Hz, 2 H, SiCH=), 6.1 (m, 4 H, =CH<sub>2</sub>) ppm. <sup>13</sup>C NMR: δ = 75.9 (*J*<sub>Si,13C</sub> = 114.8 Hz, SiC≡), 120.7 (*J*<sub>Si,13C</sub> = 21.4 Hz, ≡C), 133.0 (*J*<sub>Si,13C</sub> = 87.2 Hz, SiC=), 136.7 (=C), 28.4, 30.5 (*t*Bu) ppm. <sup>29</sup>Si NMR: δ = –23.8 ppm.

**Hydroboration of Silanes 1a–1d:** A pure sample of silane **1a** (0.73 g, 2.99 mmol) was dissolved in THF, and a twofold excess of 9-BBN (0.75 g, 5.98 mmol) was added in one portion. The reaction mixture was stirred at 23 °C for 2 h. After the reaction was complete, the solvent and other readily volatile materials were removed. The oily residue was dissolved in pentane (3 mL) and kept at r.t. After 3–4 d, colorless crystals were separated from the mother liquor. A few crystals were dissolved in C<sub>6</sub>D<sub>6</sub>, and their NMR spectroscopic data were collected; a crystal of suitable dimensions was studied by X-ray diffraction. The other spiro-silanes were prepared in the same way. Colorless crystals of spiro-silane **3c** were grown in an analogous way. The hydroboration of silane **1d**, followed by intramolecular donor–acceptor interactions, afforded **4d**. The solid powder was dissolved in CH<sub>2</sub>Cl<sub>2</sub>, and **4d** was extracted in its pure form with a Soxhlet extractor. Our attempts to grow crystals were not successful.

**3a:** Yield 96%; m.p. 220–224 °C. <sup>1</sup>H NMR (400 MHz): δ = 0.8 (ddd, *J*<sub>H,1H</sub> = 7.5, 9.5 Hz, 2 H, 4-H, 9-H), 1.0 (ddd, *J*<sub>H,1H</sub> = 2.3, 9.4 Hz, 2 H, 4-H, 9-H), 1.0 (s, 18 H, *t*Bu), 1.5, 1.6, 1.9–2.1 (m, m, m, 28 H, 9-BBN), 2.6 (m, *J*<sub>H,1H</sub> = 2.3, 7.5 Hz, 4 H, 3-H, 8-H) ppm.

**3b:** Yield 89%. <sup>1</sup>H NMR (400 MHz): δ = 1.4, 1.7, 1.7–1.9 (m, m, m, 28 H, 9-BBN), 1.1, 1.2 (m, m, 4 H, 4-H, 9-H), 2.8, 2.9 (m, m, 4 H, 3-H, 8-H), 2.0, 6.9, 7.1 (s, m, m, 14 H, 4-Me-C<sub>6</sub>H<sub>4</sub>) ppm.

**3c:** Yield 95%; m.p. 122–124 °C. <sup>1</sup>H NMR (400 MHz): δ = 1.0 (ddd, <sup>3</sup>*J*<sub>H,1H</sub> = 4.9, 9.0 Hz, <sup>2</sup>*J*<sub>H,1H</sub> = 15.5 Hz, 2 H, 5-H), 1.2 (ddd, <sup>3</sup>*J*<sub>H,1H</sub> = 3.9, 9.0 Hz, <sup>2</sup>*J*<sub>H,1H</sub> = 15.5 Hz, 2 H, 5-H), 2.7 (ddd, <sup>3</sup>*J*<sub>H,1H</sub> = 4.9, 9.0 Hz, <sup>3</sup>*J*<sub>H,1H</sub> = 18.2 Hz, 2 H, 4-H), 2.8 (ddd, <sup>3</sup>*J*<sub>H,1H</sub> = 3.9, 9.0 Hz, <sup>3</sup>*J*<sub>H,1H</sub> = 18.2 Hz, 4-H), 1.3, 1.7–1.9 (m, m, 28 H, 9-BBN), 6.8, 6.9, 7.0 (m, m, m, 6 H, C<sub>4</sub>H<sub>3</sub>S) ppm.

**4d:** Yield 92%. <sup>1</sup>H NMR: δ = 1.1, 1.3, 1.9 (m, m, m, 9-BBN, 4-H), 2.1, 2.2 (s, s, 6 H, NMe<sub>2</sub>), 2.3 (m, 2 H, 3-H), 3.0 (m, 2 H, NCH<sub>2</sub>) ppm.

**Hydroboration of Silanes 2a:** Chlorodivinylsilane **2a** (1.09 g, 5.48 mmol) was dissolved in THF, and 9-BBN (0.50 g, 4.09 mmol) was added in one portion. The reaction proceeded at r.t. After 2 h, all readily volatile materials were removed under vacuum (10<sup>–2</sup> Torr). The remaining oily compound was studied by NMR spectroscopy and identified as mixture of **6a** (major product; ca. 90%) and **7a** (minor product; ca. 10%). Then, a further amount of 9-BBN (2 equiv.) was added, and the reaction was performed under

identical conditions. The compound was worked-up, and the oily residue obtained was pure **7a** in reasonably good yield and purity (>95% by NMR spectroscopy).

**6a:** Yield 97%. <sup>1</sup>H NMR (400 MHz):  $\delta$  = 1.05 (s, 9 H, *t*Bu), 0.94 (m, 2 H, 5-H), 2.45 (m, 2 H, 4-H), 1.44, 1.57–1.96 (m, 14 H, BBN), 5.93 (dd, 1 H, SiCH), 6.06 (dd, 2 H, =CH<sub>2</sub>) ppm. <sup>13</sup>C NMR (100.5 MHz):  $\delta$  = 147.8 ( $J_{29\text{Si},13\text{C}}$  = 73.4 Hz, C-2), 171.4 (br., C-3), 33.1 (C-4), 12.2 ( $J_{29\text{Si},13\text{C}}$  = 62.0 Hz, C-5), 136.6 ( $J_{29\text{Si},13\text{C}}$  = 72.2 Hz, SiCH<sub>2</sub>), 134.9 (H<sub>2</sub>C=), 28.5 (q), 30.5 (Me, *t*Bu), 35.5, 32.7 (br), 23.7 (9-BBN) ppm. <sup>11</sup>B NMR (128.3 MHz):  $\delta$  = 85.4 ppm. <sup>29</sup>Si NMR (59.6 MHz):  $\delta$  = 24.6 ppm.

**7a:** Yield 96%. <sup>1</sup>H NMR (400 MHz):  $\delta$  = 1.21 (s, 9 H, *t*Bu), 1.27, 1.48 (m, m, 2 H, 5-H), 2.49 (m, 2 H, 4-H), 1.61–2.03 (m, SiCH<sub>2</sub>CH<sub>2</sub>, 9-BBN) ppm. <sup>13</sup>C NMR (100.5 MHz):  $\delta$  = 147.6 ( $J_{29\text{Si},13\text{C}}$  = 69.6 Hz, C-2), 171.1 (br., C-3), 33.8 (C-4), 11.3 ( $J_{29\text{Si},13\text{C}}$  = 59.5 Hz, C-5), 20.5 (br., BCH<sub>2</sub>), 13.4 ( $J_{29\text{Si},13\text{C}}$  = 56.6 Hz, SiCH<sub>2</sub>), 35.5, 32.7, 31.5 (br), 23.67, 23.65 (9-BBN), 33.7 (Me *t*Bu), 35.3 (C<sub>q</sub> *t*Bu). <sup>11</sup>B NMR (96.2 MHz):  $\delta$  = 85.4 ppm. <sup>29</sup>Si NMR (59.6 MHz):  $\delta$  = 40.9 ppm.

**Protodeborylation of 3b and 3c:** The protodeborylation and purification of **3b** and **3c** were performed by following the literature procedure.<sup>[30]</sup> Compound **5b** was dissolved in pentane (3 × 5 mL), and the solvent and all other volatiles were removed. The suspension obtained was dissolved in hot hexane and kept at 23 °C. Crystals of appropriate dimensions were grown, and their X-ray diffraction and NMR spectroscopic data were collected. Exactly the same procedure was practiced for spirosilane **5c**, except that the crystals were obtained from a solution in THF.

**5b:** Yield 82%. <sup>1</sup>H NMR (300 MHz):  $\delta$  = 0.7, 0.9 (ddd, ddd, <sup>2</sup> $J_{\text{H},\text{H}}$  = 15.6 Hz, <sup>3</sup> $J_{\text{H},\text{H}}$  = 4.8, 9.2 Hz, 4 H, 4-H, 9-H), 2.2–2.4 (m, 4 H, 3-H, 8-H), 1.9, 6.7, 7.2 (s, m, m, 14 H, 4-Me-C<sub>6</sub>H<sub>4</sub>), 6.8 (t, <sup>3</sup> $J_{\text{H},\text{H}}$  = 3.0 Hz, 2 H, 2-H, 7-H) ppm.

**5c:** Yield 87%. <sup>1</sup>H NMR (400 MHz):  $\delta$  = 0.82 (ddd,  $J_{\text{H},\text{H}}$  = 4.9, 8.9, 15.8 Hz, 2 H, 4-H), 1.05 (ddd,  $J_{\text{H},\text{H}}$  = 4.9, 8.9, 15.8 Hz, 2 H,

4-H), 2.48 (m, 4 H, 3-H), 6.84 (t,  $J_{\text{H},\text{H}}$  = 3.0 Hz,  $J_{29\text{Si},1\text{H}}$  = 12.7 Hz, 2 H, 2-H), 6.87 (dd,  $J_{\text{H},1\text{H}}$  = 2.9, 5.0 Hz, 2 H, 3-thienyl), 6.97 (m,  $J_{\text{H},1\text{H}}$  = 1.0, 2.9 Hz, 2 H, 3-thienyl) 7.08 (dd,  $J_{\text{H},1\text{H}}$  = 1.0, 5.0 Hz, 2 H, 3-thienyl) ppm.

**Silane 8a:** A Schlenk tube was charged with pure silane **7a** (1.32 g, 3.0 mmol) and hexane (10 mL). To this solution, an equimolar amount of *N*-trimethylsilylpyrazole was slowly added with constant stirring. The reaction proceeded at 23 °C and was constantly monitored by <sup>29</sup>Si NMR spectroscopy (**7a**:  $\delta$  = +40.9 ppm → **8a**:  $\delta$  = +32.1 ppm). After 4–5 h, the reaction was complete, and all readily volatile materials and solvent were removed under vacuum; the solid residue (pure **8a**) was dissolved in hot hexane (2 mL). Colorless crystals were grown after 3 d, yield 70%. <sup>1</sup>H NMR (400 MHz, CDCl<sub>3</sub>):  $\delta$  = 0.58 (s, 9 H, *t*Bu), 0.01, 0.40, 0.62, 0.93, 1.16–1.68 (m, 9-BBN, 5-H, CH<sub>2</sub>CH<sub>2</sub>), 6.86 (s, 1 H, =CH), 5.95, 7.10, 7.70 (m, m, 3 H, pyrazole) ppm. <sup>13</sup>C NMR:  $\delta$  = 147.3 ( $J_{29\text{Si},13\text{C}}$  = 67.6 Hz, C-1), 174.8 (br., C-2), 33.0 (C-3), 12.1 ( $J_{29\text{Si},13\text{C}}$  = 59.9 Hz, C-4), 7.1 ( $J_{29\text{Si},13\text{C}}$  = 59.7 Hz, SiCH<sub>2</sub>), 15.3 (br., CH<sub>2</sub>), 33.4 (Me *t*Bu), 34.8 (C<sub>q</sub>, *t*Bu), 139.7, 137.4, 105.5 (pyrazole), 35.2, 35.1, 34.4, 32.2, 32.5 (br), 31.5, 30.9, 24.8, 24.6, 23.3 (2 × BBN) ppm. <sup>15</sup>N NMR (50.7 MHz):  $\delta$  = –165.2 (SiN), –117.7 (BN) ppm. <sup>11</sup>B NMR (96.2 MHz):  $\delta$  = 85.0, –2.8 ppm. <sup>29</sup>Si NMR (59.6 MHz):  $\delta$  = 32.1 ppm.

#### Crystal Structure Determinations of Spirosilanes 3a, 3b, 5b, and 8a:

Details pertinent to the crystal structure determinations are listed in Table 3. Crystals of appropriate size were selected (in perfluorinated oil<sup>[37]</sup> at room temperature), and the data collections were performed at 133 K by using a STOE IPDS II system equipped with an Oxford Cryostream low-temperature unit. The structure solutions and refinements were accomplished by using SIR97,<sup>[38]</sup> SHELXL-97,<sup>[39]</sup> and WinGX.<sup>[40]</sup> CCDC-992918 (for **3a**), -992919 (for **3c**), -992921 (for **5b**), and -992920 (for **8a**) contain the supplementary crystallographic data for this paper. These data can be obtained free of charge from The Cambridge Crystallographic Data Centre via www.ccdc.cam.ac.uk/data\_request/cif.

Table 3. Data pertinent to the crystal structure determinations of **3b**, **3c**, **5b**, and **8a**.

	<b>3a</b> (R = <i>t</i> Bu)	<b>3c</b> (R = 3-thienyl)	<b>5b</b> (R = 4-Me-C <sub>6</sub> H <sub>4</sub> )	<b>8a</b> (R = <i>t</i> Bu)
Formula	C <sub>32</sub> H <sub>54</sub> B <sub>2</sub> Si	C <sub>32</sub> H <sub>42</sub> B <sub>2</sub> S <sub>2</sub> Si	C <sub>22</sub> H <sub>24</sub> Si	C <sub>29</sub> H <sub>48</sub> B <sub>2</sub> N <sub>2</sub> Si
Crystal shape	prism	prism	platelike	prism
Dimensions [mm]	0.62 × 0.27 × 0.18	0.56 × 0.38 × 0.32	0.34 × 0.32 × 0.09	0.62 × 0.50 × 0.34
Crystal system	triclinic	monoclinic	monoclinic	triclinic
Space group	<i>P</i> 1	<i>P</i> 2/ <i>c</i>	<i>C</i> 2/ <i>c</i>	<i>P</i> 1
<i>a</i> [pm]	1075.8(8)	670.0(5)	2253.1(9)	783.3(7)
<i>b</i> [pm]	1138.1(8)	687.7(5)	558.0(3)	1324.5(13)
<i>c</i> [pm]	1242.5(9)	3098.9(3)	1652.4(8)	1490.0(14)
$\alpha$ [°]	77.7(6)	90	90	109.8(7)
$\beta$ [°]	78.7(6)	94.0(0)	124.9(6)	102.3(7)
$\gamma$ [°]	83.7(6)	90	90	100.1(7)
<i>Z</i>	2	2	4	2
Absorption coefficient $\mu$ [mm <sup>-1</sup> ]	0.10	0.25	0.14	0.11
Diffraction	STOE IPDS II, Mo-K $\alpha$ , $\lambda$ = 71.069 pm, graphite monochromator			
Measuring range [°]	1.7–25.8	1.3–25.7	2.2–25.65	1.52–25.71
Reflections collected	19253	12539	10830	17090
Independent reflections [ $I > 2\sigma(I)$ ]	4723	2377	1328	3611
Absorption correction	none	none	none	none
Refined parameters	316	168	106	341
$wR_2/R_1$ [ $F^2 > 2\sigma(F^2)$ ]	0.110/0.057	0.139/0.057	0.161/0.056	0.101/0.044
Max./min. residual electron density [e <sup>-</sup> pm <sup>-3</sup> × 10 <sup>-6</sup> ]	0.52/–0.21	0.44/–0.32	0.45/–0.26	0.49/–0.24

## Acknowledgments

The financial support from the Higher Education Commission (HEC) Pakistan under the National Research Program for Universities (NRPU) (grant number 20-1488/R&D/09-5432) is gratefully acknowledged. The authors are also thankful to Deutscher Akademischer Austauschdienst (DAAD) and the Deutsche Forschungsgemeinschaft (DFG) for support.

- [1] a) B. Wrackmeyer, *Coord. Chem. Rev.* **1995**, *145*, 125–156; b) B. Wrackmeyer, *Heteroat. Chem.* **2006**, *17*, 188–206; c) B. Wrackmeyer, O. L. Tok, *Comprehensive Heterocyclic Chemistry III* (Eds.: A. R. Katritzky, C. A. Ramsden, E. F. V. Scriven, R. J. K. Taylor), Elsevier, Oxford, UK, **2008**, ch. 3.17, p. 1181–1223.
- [2] a) B. Wrackmeyer, O. L. Tok, E. V. Klimkina, W. Milius, *Eur. J. Inorg. Chem.* **2010**, 2276–2282; b) B. Wrackmeyer, B. H. Kenner-Hofmann, W. Milius, P. Thoma, O. L. Tok, M. Herberhold, *Eur. J. Inorg. Chem.* **2006**, 101–108.
- [3] J. Ugolotti, G. Dierker, R. Fröhlich, G. Kehr, G. Erker, *J. Organomet. Chem.* **2011**, *696*, 1184–1188.
- [4] B. Wrackmeyer, H. E. Maisel, E. Molla, A. Mottalib, A. Badshah, M. H. Bhatti, S. Ali, *Appl. Organomet. Chem.* **2003**, *17*, 465–472.
- [5] a) B. Wrackmeyer, E. Khan, R. Kempe, *Appl. Organomet. Chem.* **2007**, *23*, 39–45; b) B. Wrackmeyer, E. Khan, S. Bayer, K. Shahid, *Z. Naturforsch. B* **2007**, *62*, 1174–1182.
- [6] a) E. Khan, S. Bayer, B. Wrackmeyer, *Z. Naturforsch. B* **2009**, *64*, 47–57; b) E. Khan, B. Wrackmeyer, *Turk. J. Chem.* **2010**, *34*, 793–803; c) E. Khan, B. Wrackmeyer, *Cent. Eur. J. Chem.* **2011**, *9*, 126–132.
- [7] a) B. Wrackmeyer, O. L. Tok, R. Kempe, *Inorg. Chim. Acta* **2005**, *358*, 4183–4190; b) B. Wrackmeyer, O. L. Tok, W. Milius, A. Khan, A. Badshah, *Appl. Organomet. Chem.* **2006**, *20*, 99–105.
- [8] a) E. Khan, R. Kempe, B. Wrackmeyer, *Appl. Organomet. Chem.* **2009**, *23*, 124–131; b) E. Khan, O. L. Tok, B. Wrackmeyer, *Appl. Organomet. Chem.* **2014**, *28*, 280–285.
- [9] E. Khan, B. Wrackmeyer, *Cent. Eur. J. Chem.* **2012**, *10*, 1633–1639.
- [10] a) J. Ugolotti, G. Kehr, R. Fröhlich, G. Erker, *Chem. Commun.* **2010**, *46*, 3016–3018; b) G. Dierker, J. Ugolotti, G. Kehr, R. Fröhlich, G. Erker, *Adv. Synth. Catal.* **2009**, *351*, 1080–1088.
- [11] J. Y. Corey, in: *Aggregation-Induced Emission: Fundamentals* (Eds.: A. Qin, B. Z. Tang), Wiley, Chichester, UK, **2013**, p. 1–37.
- [12] a) E. Khan, B. Wrackmeyer, *Z. Naturforsch. B* **2009**, *64*, 1098–1106; b) E. Khan, S. Bayer, R. Kempe, B. Wrackmeyer, *Eur. J. Inorg. Chem.* **2009**, 4416–4424; c) E. Khan, S. Bayer, B. Wrackmeyer, *Z. Naturforsch. B* **2009**, *64*, 995–1002; d) B. Wrackmeyer, G. Kehr, J. Süß, E. Molla, *J. Organomet. Chem.* **1998**, *562*, 207–215; e) B. Wrackmeyer, G. Kehr, J. Süß, E. Molla, *J. Organomet. Chem.* **1999**, *577*, 82–92; f) B. Wrackmeyer, W. Milius, A. Badshah, *J. Organomet. Chem.* **2002**, *656*, 97–101; g) B. Wrackmeyer, M. H. Bhatti, S. Ali, O. L. Tok, Y. N. Bubnov, *J. Organomet. Chem.* **2002**, *657*, 146–154; h) B. Wrackmeyer, H. E. Maisel, W. Milius, M. H. Bhatti, S. Ali, *Z. Naturforsch. B* **2003**, *58*, 543–552.
- [13] a) B. Wrackmeyer, E. Khan, R. Kempe, *Z. Naturforsch. B* **2007**, *62*, 75–81; b) B. Wrackmeyer, H. E. Maisel, W. Milius, M. H. Bhatti, S. Ali, *J. Organomet. Chem.* **2003**, *669*, 72–78; c) B. Wrackmeyer, O. L. Tok, W. Milius, M. H. Bhatti, S. Ali, *Z. Naturforsch. B* **2003**, *58*, 133–138.
- [14] a) B. Wrackmeyer, K. Shahid, S. Ali, *Appl. Organomet. Chem.* **2005**, *19*, 377–382; b) B. Wrackmeyer, K. Shahid, S. Ali, *Z. Naturforsch. B* **2005**, *60*, 590–592; c) B. Wrackmeyer, E. Khan, W. Milius, *Z. Naturforsch. B* **2008**, *63*, 1267–1275.
- [15] a) R. West, *J. Am. Chem. Soc.* **1954**, *76*, 6012–6014; b) I. S. Touloukhonova, D. R. Friedrichsen, N. J. Hill, T. Müller, R. West, *Angew. Chem. Int. Ed.* **2006**, *45*, 2578–2581; *Angew. Chem.* **2006**, *118*, 2640.
- [16] a) W. J. Richter, *Synthesis* **1982**, 1102; b) R. G. Salomon, *J. Org. Chem.* **1974**, *39*, 3602; c) V. Dejean, H. Gornitzka, G. Oba, M. Koenig, G. Manuel, *Organometallics* **2000**, *19*, 711–713.
- [17] a) K. Tamao, K. Nakamura, H. Ishii, S. Yamaguchi, M. Shiro, *J. Am. Chem. Soc.* **1996**, *118*, 12469–12470; b) D. Terunuma, S. Hata, T. Araki, T. Ueki, T. Okazaki, Y. Suzuki, *Bull. Chem. Soc. Jpn.* **1977**, *50*, 1545–1548.
- [18] a) E. A. Chernyshev, S. A. Bashkirova, A. B. Petrunin, P. M. Matveichev, V. M. Nosova, *Metalloorg. Khim.* **1991**, *4*, 378–383; b) Y. T. Park, S. Q. Zhou, G. Manuel, W. P. Weber, *Macromolecules* **1991**, *24*, 3221–3226.
- [19] D. Yan, J. Mohsseni-Ala, N. Auner, M. Bolte, J. W. Bats, *Chem. Eur. J.* **2007**, *13*, 7204–7214.
- [20] B. Wrackmeyer, E. Khan, R. Kempe, *Appl. Organomet. Chem.* **2008**, *22*, 383–388.
- [21] E. Khan, B. Wrackmeyer, R. Kempe, *Eur. J. Inorg. Chem.* **2008**, 5367–5372.
- [22] W. E. Davidssohn, M. C. Henry, *Chem. Rev.* **1967**, *67*, 73–106.
- [23] a) L. Brandsma, *Preparative Acetylenic Chemistry*, 2nd ed., Elsevier, Amsterdam, **1988**; b) L. Brandsma, *Synthesis of Acetylenes, Allenes, and Cumulenes – Methods and Techniques*, Elsevier, Amsterdam, **2004**.
- [24] a) B. Wrackmeyer, E. Khan, S. Bayer, O. L. Tok, E. V. Klimkina, W. Milius, R. Kempe, *Z. Naturforsch. B* **2010**, *65*, 725–744; b) B. Wrackmeyer, E. Khan, A. Badshah, E. Molla, P. Thoma, O. L. Tok, W. Milius, R. Kempe, J. Senker, *Z. Naturforsch. B* **2010**, *65*, 119–126.
- [25] Y. Xia, Y. Li, W. Li, *J. Organomet. Chem.* **2008**, *693*, 2722–2728.
- [26] a) H. C. Brown, A. W. Moerikofer, *J. Am. Chem. Soc.* **1963**, *85*, 2063–2065; b) C. A. Brown, R. A. Coleman, *J. Org. Chem.* **1979**, *44*, 2328–2329.
- [27] T. Parella, *J. Magn. Reson.* **2004**, *167*, 266–272.
- [28] B. Wrackmeyer, *Prog. Nucl. Magn. Reson. Spectrosc.* **1979**, *12*, 227–259.
- [29] a) A. Suzuki, in: *Modern Arene Chemistry* (Ed.: D. Astruc), Wiley-VCH, Weinheim, Germany, **2002**, p. 53–106; b) N. Miyaoura, A. Suzuki, *Chem. Rev.* **1995**, *95*, 2457–2483.
- [30] B. Wrackmeyer, E. Khan, R. Kempe, *Z. Naturforsch. B* **2008**, *63*, 275–279.
- [31] a) A. D. Becke, *J. Chem. Phys.* **1993**, *98*, 5648–5652; b) C. Lee, W. Yang, R. G. Parr, *Phys. Rev. B* **1988**, *41*, 785–789; c) P. J. Stevens, F. J. Devlin, C. F. Chabrowski, M. J. Frisch, *J. Phys. Chem.* **1994**, *98*, 11623–11627; d) D. McLean, D. G. S. Chandler, *J. Chem. Phys.* **1980**, *72*, 5639–5648; e) R. Krishnan, J. S. Binkley, R. Seeger, J. A. Pople, *J. Chem. Phys.* **1980**, *72*, 650–654.
- [32] K. Wollinski, J. F. Hinton, P. J. Pulay, *J. Am. Chem. Soc.* **1990**, *112*, 8251–8260.
- [33] a) T. Helgaker, M. Jaszunski, M. Pecul, *Prog. Nucl. Magn. Reson. Spectrosc.* **2008**, *53*, 249–268; b) R. H. Contreras, V. Barone, J. C. Facelli, J. E. Peralta, *Annu. Rep. NMR Spectrosc.* **2003**, *51*, 167–260; c) R. H. Contreras, J. R. Cheeseman, M. J. Frisch, G. E. Scuseria, *Chem. Phys. Lett.* **2003**, *375*, 452–458.
- [34] M. Bühl, P. v. R. Schleyer, *J. Am. Chem. Soc.* **1992**, *114*, 477–491.
- [35] B. Wrackmeyer, *Annu. Rep. NMR Spectrosc.* **2006**, *57*, 1–49.
- [36] M. J. Frisch, G. W. Trucks, H. B. Schlegel, G. E. Scuseria, M. A. Robb, J. R. Cheeseman, G. Scalmani, V. Barone, B. Mennucci, G. A. Petersson, H. Nakatsuji, M. Caricato, X. Li, H. P. Hratchian, A. F. Izmaylov, J. Bloino, G. Zheng, J. L. Sonnenberg, M. Hada, M. Ehara, K. Toyota, R. Fukuda, J. Hasegawa, M. Ishida, T. Nakajima, Y. Honda, O. Kitao, H. Nakai, T. Vreven, J. A. Montgomery Jr., J. E. Peralta, F. Ogliaro, M. Bearpark, J. J. Heyd, E. Brothers, K. N. Kudin, V. N. Staroverov, T. Keith, R. Kobayashi, J. Normand, K. Raghavachari, A. Rendell, J. C. Burant, S. S. Iyengar, J. Tomasi, M. Cossi, N.

- Rega, J. M. Millam, M. Klene, J. E. Knox, J. B. Cross, V. Bakken, C. Adamo, J. Jaramillo, R. Gomperts, R. E. Stratmann, O. Yazyev, A. J. Austin, R. Cammi, C. Pomelli, J. W. Ochterski, R. L. Martin, K. Morokuma, V. G. Zakrzewski, G. A. Voth, P. Salvador, J. J. Dannenberg, S. Dapprich, A. D. Daniels, O. Farkas, J. B. Foresman, J. V. Ortiz, J. Cioslowski, D. J. Fox, Gaussian09, revision A.02, Gaussian, Inc., Wallingford CT, **2010**.
- [37] T. Kottke, D. Stalke, *J. Appl. Crystallogr.* **1993**, *26*, 615–619.
- [38] A. Altomare, M. C. Burla, M. Camalli, G. L. Cascarano, C. Giacovazzo, A. Guagliardi, A. G. G. Moliterni, G. Polidori, R. Spagna, *J. Appl. Crystallogr.* **1999**, *32*, 115–119.
- [39] G. M. Sheldrick, *SHELX-97, Program for Crystal Structure Analysis* (release 97-2), Institut für Anorganische Chemie der Universität Göttingen, Germany, **1998**.
- [40] L. J. Farrugia, *J. Appl. Crystallogr.* **1999**, *32*, 837–838.

Received: April 9, 2014  
Published Online: June 16, 2014